

Research Article

The effect of Sulforaphane on perinatal hypoxic-ischemic brain injury in rats

Kapoor, S^{1,2}, Kala, D.², Svoboda, J.², Daněk, J.², Faridová, A.², Brnoliaková, Z.¹, Mikulecká, A.², Folbergrová, J.², Otáhal, J.^{2,3}

¹ *Institute of Experimental Pharmacology and Toxicology, Centre of Experimental Medicine, Slovak Academy of Sciences, Bratislava, Slovak Republic*

² *Institute of Physiology, Czech Academy of Sciences, Prague, Czech Republic*

³ *Department of Pathophysiology, Second Faculty of Medicine, Charles University, Prague, Czech Republic*

· Corresponding author to e-mail: jakub.otahal@fgu.cas.cz

Summary: (250 Words)

Perinatal hypoxic-ischemic insult (HII) is one of the main devastating causes of morbidity and mortality in newborns. HII induces brain injury which evolves to neurological sequelae later in life. Hypothermia is the only therapeutic approach available capable of diminishing brain impairment after HII. Finding a novel therapeutic method to reduce the severity of brain injury and its consequences is critical in neonatology. The present paper aimed to evaluate the effect of sulforaphane (SFN) pre-treatment on glucose metabolism, neurodegeneration, and functional outcome at the acute, sub-acute, and sub-chronic time intervals in the experimental model of perinatal hypoxic-ischemic insult in rats. To estimate the effect of SFN on brain glucose uptake we have performed 18F-deoxyglucose (FDG) μ CT/PET. The activity of FDG was determined in the hippocampus and sensorimotor cortex. Neurodegeneration was assessed by histological analysis of Nissl-stained brain sections. To investigate functional outcomes a battery of behavioral tests was employed. We have shown that although SFN possesses a protective effect on glucose uptake in the ischemic hippocampus 24hr and 1 Wk after HII, no effect has been observed in the motor cortex. We have further shown that the ischemic hippocampal formation tends to be thinner in HIE and SFN treatment tends to reverse this pattern. We have observed subtle chronic movement deficit after HII detected by ladder rung walking test with no protective effect of SFN. SFN should be thus considered as a potent neuroprotective drug with the capability to interfere with pathophysiological processes triggered by perinatal hypoxic-ischemic insult.

Keywords: Perinatal hypoxic-ischemic insult (HII), rat, FDG-PET, Sulforaphane, neuronal damage, motor impairment

Introduction

Hypoxic-ischemic encephalopathy (HIE) is a brain injury occurring as a result of a hypoxic-ischemic insult (HII) during the prenatal, intrapartum, or postnatal period [1]. According to WHO, neonatal asphyxia, the main cause of hypoxic-ischemic encephalopathy in full-term infants, is one of the leading causes of neonatal deaths within the first week of life [2]. After the birth, an initial period is crucial for the newborns as 15-20% of HII sufferers die, and surviving infants develop neurological sequelae later in life such as cerebral palsy, epilepsy, developmental delay, cognitive impairment, and behavioral disorders [3]. HIE is one of the most common etiologies of acute symptomatic seizures in the perinatal period and the cause of epilepsy later in life [4]. Globally, there are up to 1.2 million deaths and almost 1.15 million neonates have some form of central nervous system (CNS) dysfunction each year due to HIE [3].

Basal ganglia, thalamus, internal capsule, cortex, subcortical and periventricular white matter, and medial temporal lobe are the usual sites of brain injury in HII and form a neuropathological pattern of periventricular leukomalacia [5]. HII affects the brain by disrupting various processes on both cellular and subcellular level including, cellular signaling, neurotransmission, neural connectivity and function, developmental apoptosis, and mitochondrial dysfunction [6].

Neonatal HII is the combination of the decrease in oxygen supply (hypoxia) and cerebral blood flow (ischemia) which results and provokes a cascade of biochemical changes that leads to neuronal cell death and brain damage [7]. The pathologic events of HIE are a result of impaired cerebral blood flow and oxygen delivery to the brain. The pathophysiology of HII is complex and evolves with two distinct phases of energy failure [1]. In primary energy failure, the impairment of cerebral blood flow causes a reduction in oxygen and nutrient supply leading to significantly less production of adenosine triphosphate and phosphocreatine, and metabolism finally switches to anaerobic metabolism and increased lactate production. The secondary energy failure occurs after 6 to 48 hours of the primary injury and the mechanism appears to be linked to oxidative stress, inflammation, and consequences of excitotoxicity [8 - 10].

Oxidative stress and mitochondrial dysfunction have been implicated in the pathogenesis of many neurological disorders in adults [11 - 13].

We have shown recently that oxidative stress is present also in the immature brain during experimentally induced status epilepticus and is the cause of lasting metabolic dysfunction [14].

Oxidative stress and mitochondrial damage have been also implicated in the pathogenesis of HIE [15, 16]. There is a continuous demand for antioxidants to prevent or balance oxidative stress in favor of re-establishing an equilibrium redox state [17]. Endogenous antioxidative systems act either as free radical scavengers or inducers of endogenous antioxidative systems, finally preventing or repairing damages caused by reactive oxygen species (ROS) and reactive nitrogen species (RNS). Oxidative stress-mediated by mitochondria, disrupt calcium homeostasis, and apoptosis, and plays a significant role in the etiology of primary and secondary energy failure in HIE [18].

Sulforaphane (SFN), an extract from broccoli, activates the KEAP1-Nrf2-ARE pathway leading to the induction of an endogenous antioxidative system [19, 20].

SFN has the potential role in the management of diseases in which chronic oxidative stress plays a major etiological role [21, 22]. Activation of the transcription factor, Nrf2 (nuclear factor-erythroid 2-related factor 2) is one of the major cellular defense lines against oxidative stress [23]. Nrf2 induces the expression of Nrf2-dependent enzymes of the antioxidant system in which cells respond to oxidative stress, such as heme oxygenase-1 (HO-1), superoxide dismutase, catalase, NAD(P)H:quinone oxidoreductase 1, glutathione reductase, and glutathione peroxidase [24]. The effect of Nrf2 on gene expression including the antioxidative system is thoroughly described in several reviews [25]. However, SFN has been found to possess other beneficial mechanisms of action such as mTOR inhibition [26] and interaction with neurovascular coupling [27].

The only available intervention in neonatal HII is therapeutic hypothermia [28], within the first 6 hours of the window after birth [29]. The latest study indicates that current treatment is only partially effective, and infants still suffer from severe brain damage and neurological impairments [30]. Hence, there is an urgency to find a novel therapeutic intervention that diminishes brain injury and neurological sequelae in new-born.

The present paper aimed to evaluate the hypothesis that sulforaphane has a beneficial effect on the brain affected by HII. We, therefore, assessed the effect of SFN pre-treatment on glucose metabolism at the acute, sub-acute, and sub-chronic time intervals, neurodegeneration, and final functional outcome in the experimental model of perinatal hypoxic-ischemic insult in rats.

Methods

Animals and SFN pretreatment

In this experiment, 6-days old Sprague-Dawley rat pups (Charles River, Germany, n= 24 male; n=12 female) were used (~18 g weight). The protocol of the experiment was approved by the Animal care and use committee of the Institute of Physiology, Czech Academy of Sciences. Animals were randomly divided into 4 groups – sham-operated (SHAM, n=4), sham-operated with SFN treatment (SHAM+SFN, n=4), hypoxic-ischemic insult (HIE, n=8), and hypoxic-ischemic insult with SFN treatment (HIE+SFN, n=8). On postnatal day 6, Sulforaphane (APExBIO, USA) was administered intraperitoneally in dose 5mg/kg (SHAM+SFN, HIE+SFN). Sulforaphane was diluted in 0.9% NaCl containing 0.5% (v/v) dimethyl sulfoxide.

Control animals received corresponding volumes (0.01ml of the solution per gram of the body weight) of the appropriate vehicles.

Surgery

Seven days old rat pups were chosen for this experiment for their level of brain maturation which is comparable to human newborns [31]. The rat pups were removed from their dams 1 h before the surgery. Briefly, perinatal HII was induced in seventh-day-old rat pups according to the modified Rice - Vannucci model [32]. Briefly, the animals were anesthetized in an inducing chamber using 3-4% of isoflurane. Subsequently, the animal's

anesthesia was maintained with 1-2% of Isoflurane and controlled throughout the surgery. The left common carotid artery (CCA) was ligated (visually confirmed occlusion) and a surgical suture was used to close the skin incision. Pups were left with dams to recover for 90 minutes. Animals were incubated in a normobaric hypoxic chamber for 90 minutes in humidified air (pO₂ 8%) and the temperature of the nest was controlled by an automatic heating pad. The SHAM groups underwent the same procedure, however, the left common carotid artery only was isolated without its ligation and animals did not undergo hypoxia.

18F-DG scanning

Microscopic computed tomography and positron emission tomography (μ CT/PET) scans were performed in the animals at the three different periods after 24hr, 1 week (1 Wk), and 5 weeks (5 Wk) after HII.

To assess changes in glucose metabolism, a small animal PET scanning device with a spatial resolution of up to 0.7mm was used (Albira, Bruker, USA). FDG (18F-DG; ÚJV, Czech Republic) has been used in our experiments. Animals were intravenously injected (jugular vein) with the selected dose of FDG (10–15 MBq for PD8 and PD13 animals, and 18-20 MBq for PD42 animals) dissolved in saline to a total volume of 200 or 400 μ l (PD42), while shortly anesthetized by isoflurane.

We waited 45 minutes after the FDG dosage administration for the FDG uptake into the brain [33]. Finally, the animals were re-anesthetized with isoflurane and placed into the scanner for detection of FDG activity. The PET scan took 45 minutes for each animal followed by a 10 minutes CT acquisition sequence. The offline data analysis was performed using PMOD 3.6.1 (PMOD technologies LLC, Zurich, Switzerland). Co-registration of the PET scan with Schiffer's MRI rat brain atlas [34] implementing the PET scan into Paxinos coordinates was performed by trained specialists. FDG activity was assessed in the individual brain regions according to the stereotactic atlas [35].

To evaluate FDG activity in the hippocampus (Hip) and motor cortex (MCx) macro-regions consisting of previously selected regions of interest (ROIs), were established by integrating activity from corresponding subregions obtained from stereotactic atlas and normalized to whole brain FDG uptake. We chose a standardized uptake value (SUV) generated by PMOD to measure variations in glucose uptake. The following formula is used by PMOD software to calculate SUV:

$$SUV = A \times W \times VD [g]$$

With the variables being: A – Activity concentration in the image (kBq/cc); D – Applied dose (kBq) at the time the image is corrected to; W – animal weight (g); V – ROI volume (cc).

Histology

To evaluate neuropathologic consequences of the hypoxic-ischemic insult animals were 5 weeks after the HII euthanized with urethane (2mg/kg, i.p.), transcardially perfused, brains removed, and processed for histology.

Tissue processing

Firstly, buffered saline (0.1M phosphate buffer, pH 7.4) was used for transcardial perfusion followed by fixation with fresh ice-cold 4% paraformaldehyde. The brain was removed from the skull and left in 4% paraformaldehyde overnight for post-fixation. After fixation, the brains were cryoprotected in sucrose solutions (10, 20, and 30%) for at least 24 hr in each concentration. Brains were quickly frozen in dry ice and cut to 50µm thick slices on cryocut (Leica).

Nissl staining

The mounted brain tissue sections were dehydrated in ethanol (70%, 80%, 90%) for 2 min each and then stained with Nissl solution (1 % cresyl violet, 0.2 mol/l acetic acid, and 0.2 mol/l sodium acetate, 4:1, pH=3) for approximately 20 min. After the visibility of desired intensity of color, the slices were washed twice in distilled water and rehydrated with ethanol (90%, 80%, 70%) for 2 min each. The slides were drenched in xylene for 5 min. Followingly, the slides were incubated in another xylene bath and were mounted with Canada balsam (Merck, Czech Republic). The histological slides were assessed under the light microscope (Olympus BX53, Japan) and morphological measurements of the hippocampus and cortex were performed using ImageJ software. Briefly, 6 perpendicular lines were placed on designated positions over sensorimotor cortex or hippocampus on each hemisphere on 10 consecutive slices (each 5th in series) in the rostrocaudal interval 1mm rostral to bregma and 3.5mm caudal to bregma. Obtained thicknesses were averaged separately for both hemispheres and structures.

Behavioral tests

To assess the cognitive and motor impairments after HII, different behavioral tests were performed at postnatal day 19 (PND 19):

Bar holding test

This test is for the assessment of the animal's ability to hold on to the front limbs and to pull the lower limbs. An animal was held by the nape and its forepaws were allowed to touch a wooden bar (25 cm long, 1 cm in diameter, suspended 25 cm above a padded soft surface). Time of successful grasping was recorded with a limit of 60s.

Open field test velocity & distance moved

This test is used to measure emotional states like anxiety in rats. The open field (OP) test was performed in a square arena (45*45*30 cm), with a camera installed above the center. Immediately after a rat was placed in the center of the arena; locomotor behavior was recorded automatically by a computerized system (Ethovision, Noldus, Netherlands) for 5 min. The software monitored the actual movement of the animal by detection method based on body-centered contrast subtracted from the background. Locomotor activity expressed as distance moved (cm) was calculated. To reduce any lingering olfactory cues all devices were cleaned after each rat was tested.

Rotarod test

To assess motor function an automatic rotarod treadmill unit (Rota-Rod advanced; TSE Systems, Bad Homburg, Germany) was used. The rats were placed individually on the rotating rod with their heads directed against rotation. Two trials were performed in close succession. The Maximum score in maintaining equilibrium was arbitrarily fixed at the 60s. The animals were tested at two speeds: 20 rotations per minute (rpm) and 30 rotations per minute (rpm). The latency to fall was measured automatically with a limit of 60s.

The ladder rung walking test

The ladder walking test was used to assess motor function and can be used specifically for assessment of skilled walking, forelimb and hind limb placing, stepping, inter-limb coordination, and balance [36]. In the present study, we used to assess the ability of rats to successfully cross the runway. A horizontal ladder walking apparatus that consisted of sidewalls made of clear Plexiglas distance of 1 cm between rungs was used. The ladder was elevated 30 cm above the ground with an empty starting cage and a refuge (home cage) at the end. The width of the alley was adjusted to the size of the animal, to prevent the animal from turning around. The time to cross the runway and the number of foot (slips) errors in one trial with regular gaps and another trial with irregular gaps were assessed. For the regular arrangement, the rungs were spaced at 2 cm intervals. For the irregular pattern, the distance of the rungs varied randomly from 1 to 5 cm.

Statistical Methods

All data were statistically analyzed in Sigmaplot software and data were expressed as mean \pm SEM. The level of statistical significance was set to 0.05. To reveal statistical difference one-way ANOVA, or paired tests (t-test or rank-sum test) were used when appropriate.

Results

Animals body weight

All animals were weighed systematically for the first 2 weeks after HII (from the PND 7 to PND 19). The weight of the animals in the four groups did not substantially differ (**Fig. 1**).

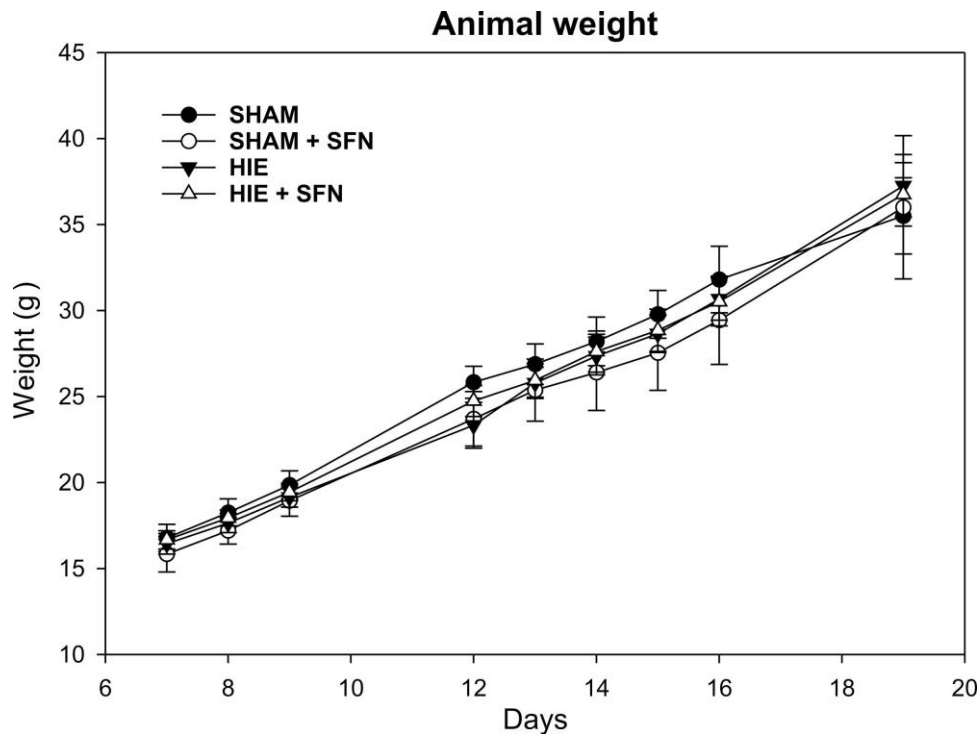


Fig. 1. Animal body weight did not differ between experimental groups. SHAM (n=4), SHAM+SFN (n=4), HIE (n=8) and HIE+SFN (n=8). Data are expressed as mean \pm SEM. * $p < 0.05$ was considered as statistical significance.

FDG μ CT/PET scanning

Cerebral glucose metabolism was evaluated by μ CT/PET scan with FDG at different time intervals – acute, sub-acute, and the sub-chronic period after HII in all experimental groups. FDG activity was analyzed in different brain regions using MRI atlas after space anatomical registration of PET and CT images.

SFN protective effect on glucose uptake in ischemic hippocampus 24hr, and 1 Wk after HII

FDG uptake was evaluated in the hippocampus after 24 hours, 1 week, and 5 weeks of HII. HII decreases glucose uptake metabolism in the ischemic hippocampus 24h and 1W after HII when compared to contralateral ROIs (**Fig. 2**). We further have observed a trend to protect the hippocampus as revealed by contra- versus ipsilateral difference 24 hours (P 0.055) and 1 week (P 0.178) after HII in the HIE+SFN and HIE group respectively. However, the SFN effect was completely withdrawn or even opposite in the HIE+SFN group after 5 weeks of HII.

FDG uptake in hippocampus

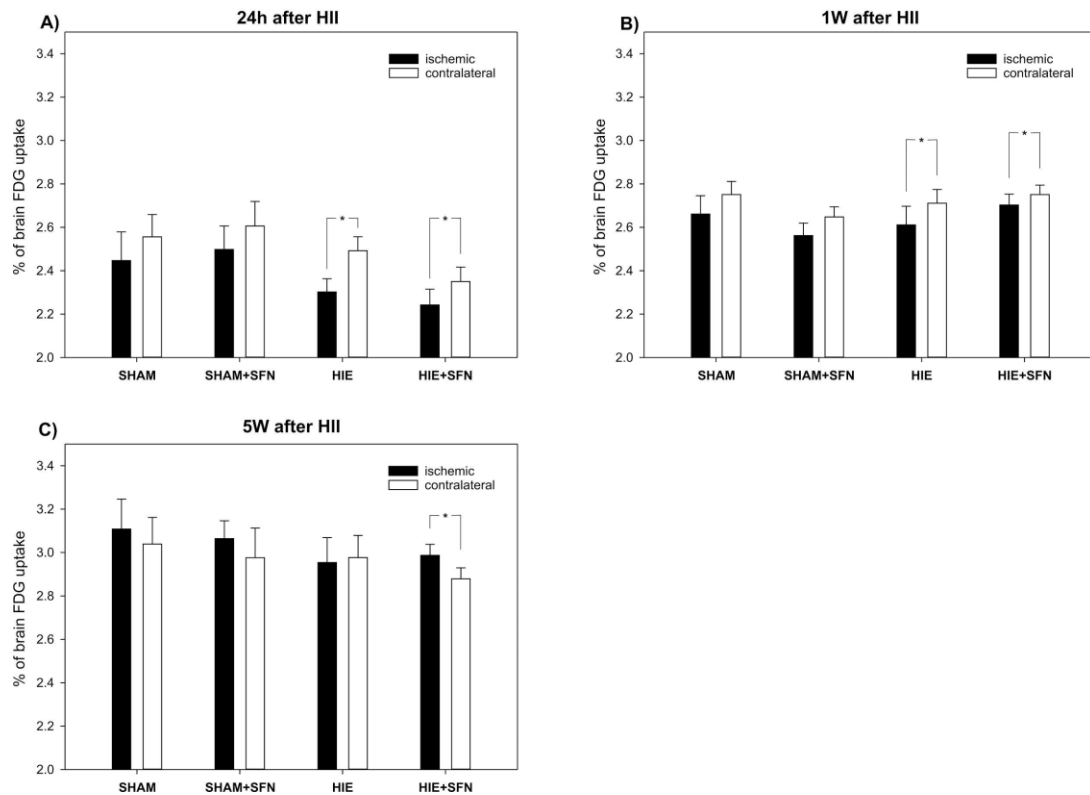


Fig. 2. FDG uptake in the hippocampus after HII. We observed a significant decrease of FDG activity in both HIE and HIE+SFN groups 24h (A) and 1W (B) after HII while 5W (C) after HII we detected a significant increase in FDG activity in the ischemic hippocampus. Data are expressed as mean \pm SEM, * $p < 0.05$.

SFN has no protective effect on glucose uptake in the motor cortex after HII

FDG uptake in the motor cortex was evaluated 24 hours, 1 week, and 5 weeks after HII. Contrary to the hippocampus we did not observe significant changes in FDG uptake within the motor cortex except the acute interval when treated with SFN. There was a statistically significant decrease in the ipsilateral motor cortex in the HIE+SFN group 24 hr after the HII (Fig. 3). However, there was no effect of SFN observed in all groups and intervals after the HII.

FDG uptake in motor cortex

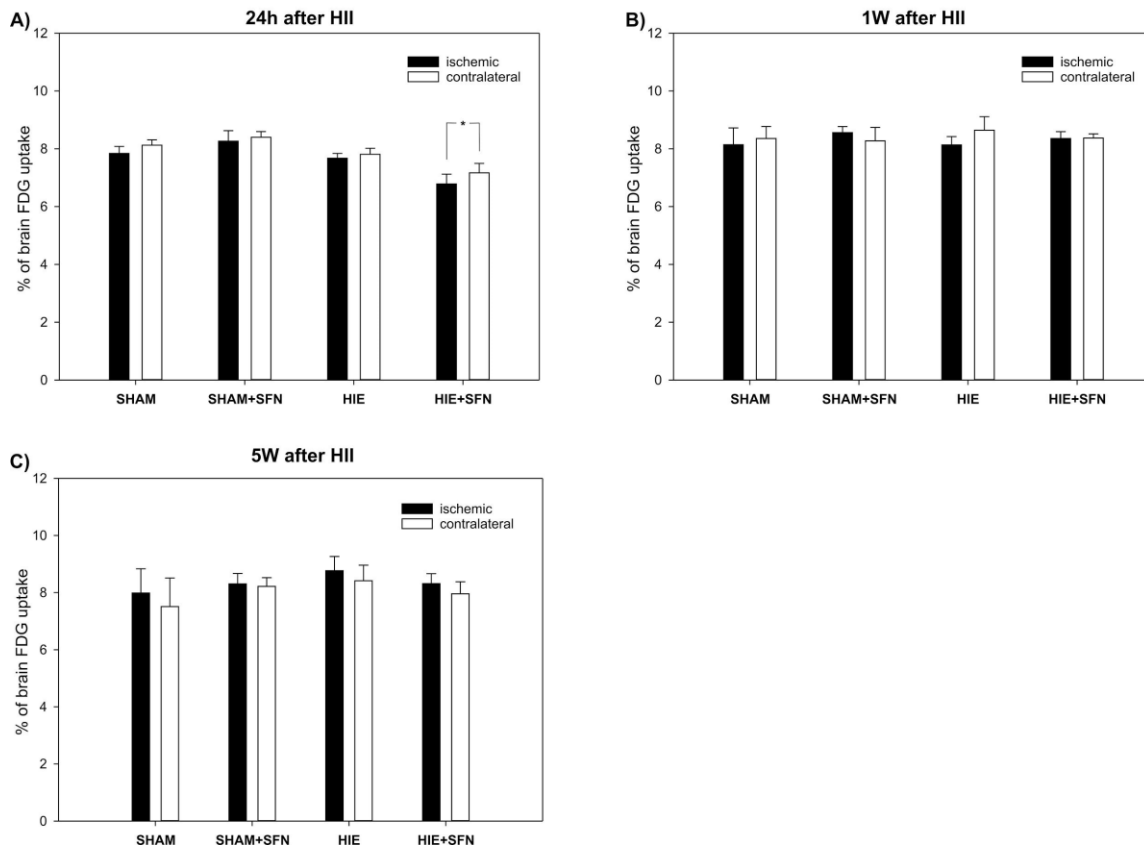


Fig. 3. FDG uptake in the motor cortex after the HII. SFN had no effect on FDG uptake except the HIE+SFN group where a significant decrease ($P < 0.05$) in the ipsilateral motor cortex has been detected (A). FDG uptake did not differ at 1 week (B) or 5 weeks (C) after the HII in all experimental groups. Data were expressed as mean \pm SEM, * $p < 0.05$.

Histology

Morphology of the brain was determined under the light microscope systematically in cortical regions and hippocampal formation on brain slices stained with Nissl stain. No obvious signs of acute degeneration or marked brain damage have been detected. We did not observe pyknotic cells or regions with loss of Nissl staining. However, enlarged lateral ventricles hinted at changes in the thickness of either the hippocampus, cortex or both. Therefore, we measured the thickness of the cortex and hippocampal formation systematically.

Ischemic hippocampal formation tended to be thinner in HIE and SFN treatment tended to reverse hippocampal impairment

Morphometric analysis of the thickness of hippocampal formation and sensorimotor cortex revealed important alterations 5 weeks after the HII. The ischemic hippocampus tended to be thinner than contralateral in the HIE group. Although the P-value has been calculated to 0.056, the finding seems to be relevant to HII. SFN treatment, however, tended to reverse hippocampal impairment ($P = 0.051$, Fig. 4.) To reveal whether the thickness of either the hippocampus or cortex determines FDG activity measured at 5 weeks interval a Pearson correlation test was performed. We did not identify any dependency between thickness and FDG activity.

Thickness of brain structures

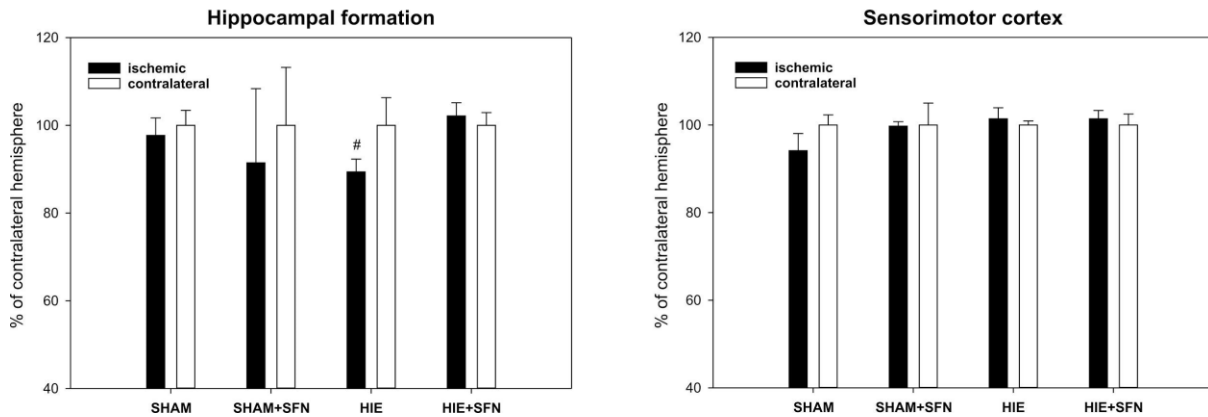


Fig. 4. The thickness of brain structures 5 weeks after the HII. Hippocampal formation tends to be thinner compared to the contralateral hemisphere in the HIE group ($P = 0.056$). SFN treatment tends to protect hippocampal formation since the interhemispheric difference in hippocampal thickness in HIE+SFN is almost normal ($P=0.607$) and differs from the HIE group ($P=0.051$). Data are expressed as mean \pm SEM, # $p<0.01$.

Behavioral Tests

To assess the influence of SFN on functional outcome after HII a set of behavioral tests has been performed. General motor activity has been assessed by Open Field test, motor performance on forced tests namely bar holding test, rotarod test, and ladder rung walking test 19 days after HII.

HII nor SFN had no effect on the open field, bar holding, and rotarod tests

Animals placed into open field arena did not differ by means of their spontaneous movement between groups in either parameter. We assessed the distance moved during the first 5 minutes of observation and the average velocity of animal movement within this period. SHAM-operated animals traveled 899.9 ± 147.2 cm with an average speed of 3 ± 0.5 cm/s. Animals from the SHAM+SFN group traveled 950.9 ± 251.5 cm with an average speed of 3.2 ± 0.8 cm/s. Animals who experienced HII (HIE and HIE+SFN) did not differ from control groups nor between them. They traveled 1041.1 ± 102.9 cm with a speed of 3.48 ± 0.3 cm/s (HIE) and 997.3 ± 157 cm with a speed of 3.3 ± 0.5 respectively.

Assessment of muscle force and endurance with bar holding test also did not reveal differences between experimental groups. Animals successfully held the bar for 29.2 ± 12.6 s in the SHAM group, 43 ± 17 s in the SHAM+SFN group, 48.7 ± 7.5 s in the HIE group, and 31.2 ± 8 s in the HIE+SFN group.

Rotarod performance test also did not detect any significant differences between experimental groups in the duration animals stayed on the rod at both rotation speeds (15 and 30 rpm). Animals stayed on the rod for 45.2 ± 7.1 s at 15rpm and 49.4 ± 6.7 s at 30rpm (SHAM), 47.3 ± 12.7 s at 15rpm and 50 ± 10 s at 30 rpm (SHAM+SFN), 53.4 ± 3.3 s at 15rpm and 52.4 ± 5.9 at 30 rpm (HIE), and 43.8 ± 7 s at 15rpm and 46.3 ± 7.2 at 30 rpm (HIE+SFN).

HII induced subtle chronic movement deficit detected by ladder rung walking test with no effect of SFN

A ladder rung walking test has been developed to detect subtle movement deficits in rodents. We performed this test in both rung settings - regular and irregular. We have observed a significant difference in the time, animals need to cross the ladder with irregular rung placement in both ischemic groups. However, we did not observe the effect of SFN treatment on ladder rung walking test performance (Fig. 5).

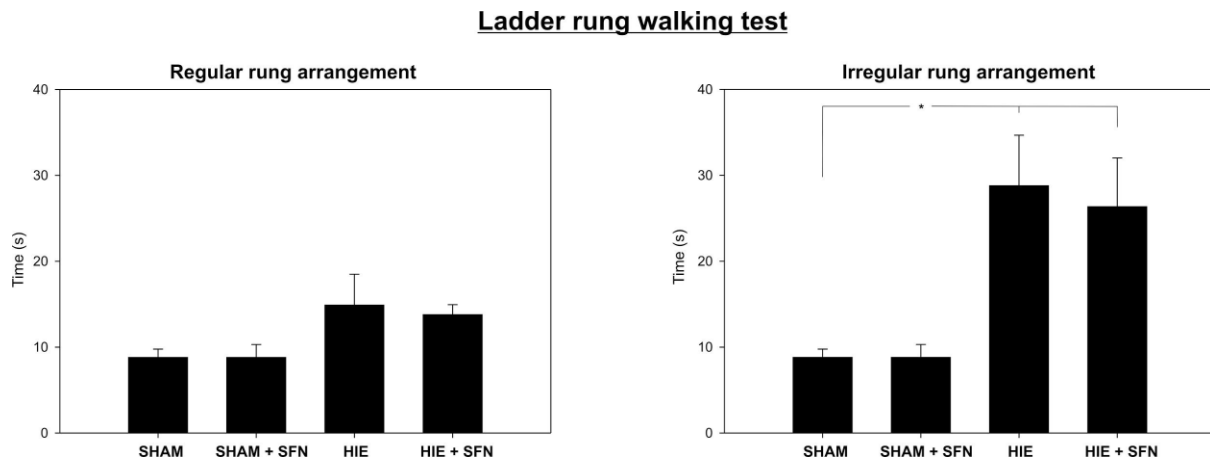


Fig. 5. Motor performance 19 days after HII. Ladder rung walking test with irregular rung arrangement revealed a significant decline in motor performance in both HIE groups with no effect of SFN. Data are expressed as mean \pm SEM, * $p < 0.05$.

Discussion

The main objective of this study was to examine the potential neuroprotective effect of SFN, a molecule showing promising clinical potential [37], in the immature brain after perinatal hypoxic-ischemic insult. In the present study, we evaluated the effect of pretreatment with SFN on glucose metabolism at the acute, sub-acute, and sub-chronic time intervals by FDG μ CT/PET scanning, neuropathology alterations to the hippocampus and sensorimotor cortex on Nissl staining, and functional outcome by a set of behavioral tests in the experimental model of perinatal hypoxic-ischemic insult in rats. We have shown that although SFN possesses a protective effect on glucose uptake in the ischemic hippocampus 24hr and 1 Wk after HII, no effect has been observed in the motor cortex. We have further shown that the ischemic hippocampal formation tends to be thinner in HIE and SFN treatment tends to reverse this pattern. We have observed subtle chronic movement deficit in HIE animals detected by ladder rung walking test with no protective effect of SFN.

We have observed decreased glucose uptake in the ischemic hippocampus 24 hours and 1 week after the hypoxic-ischemic insult. This finding is in agreement with an animal study showing decreased glucose metabolism by FDG PET in newborn pigs after cerebral hypoxia and resuscitation [38]. Dynamic FDG PET allowed the detection of cerebral metabolic rates of glucose before and early after the insult. Similar findings have been published also for hypoxic-ischemic insult in immature rats by the 2-deoxyglucose method [39], however, the authors have observed an early acute increase in glucose metabolism with consequent and lasting decrease when compared to the contralateral side. Vanucci et al. (1994) performed a time series of autoradiographic 2-deoxyglucose measurements after hypoxic-ischemic insult in immature rats with similar findings. Early increased glucose uptake is followed by normalization and lasting decrease glucose uptake starting 24 hours after the insult [40]. FDG PET has been used to assess glucose metabolism also in impaired human infants showing a strong correlation between the severity of brain injury and decline in glucose uptake 24 hours after the insult [41].

Decreased glucose uptake is a typical postischemic pattern also in an experimental model of stroke in adult rats [42]. Impairment in glucose metabolism in the ischemic hippocampus correlates well with our observation of its decreased volume as revealed by histology. In agreement with results of the thickness of the hippocampus and sensorimotor cortex is data published by Lastůvka et al. (2020) where he observed the hippocampus to be affected more

severely than the cortex by HII in mice [43]. They further found deficits in rearing and climbing after neonatal HII evaluated in adult mice. This finding is in agreement with our observation on ladder rung walking tests. Although we did not observe a difference with regular rung arrangement, a more demanding irregular rung arrangement revealed significant prolongation of animal performance. The ladder rung walking test is a sensitive assay to elaborate distinct aspects of motor function and to determine even subtle loss of movement capacity. The ladder rung walking task allows discrimination between subtle disturbances of motor function by combining qualitative and quantitative analysis of skilled walking [36], even in the later age, when the hypoxic animals show excellent recovery, the difference in the motor performance can be detected by this test [44].

We observed a protective effect of SFN pretreatment on the ischemic hippocampus by means of glucose uptake 24 hours and 1 week, and its volume as revealed by Nissl stain 5 weeks after the HII. As the most relevant cellular target of SFN action has been identified Nrf2 factor, a regulator of cellular oxidant resistance, which regulates the physiological and pathological effects of oxidant exposure by modulating the basal and induced expression of an array of ARE-dependent genes [24]. Nrf2 regulates the expression of key antioxidant system components such as glutathione and thioredoxin, as well as enzymes involved in NADPH regeneration, ROS and xenobiotic detoxification, and heme metabolism, and thus plays a critical role in cellular redox homeostasis [25]. Neuroprotective properties of SFN that have been shown to partially prevent neurodegeneration in both in vitro and in vivo conditions are extensively reviewed elsewhere [20, 45, 46]. SFN provided a neuroprotective effect in rodent models of ischemic or hemorrhagic focal cerebral ischemia where SFN significantly reduced brain infarct volume in adult animals [47, 48]. Limited data, however, exist on the SFN action in the immature brain. We have shown recently successful activation of Nrf2 and consequent induction of Nrf2 dependent antioxidative enzymes 24h after SFN application at PND11 leading to significant protection of energy metabolism after pilocarpine SE in rats [49]. Interestingly, pretreatment with SFN as early as 30 minutes before HII has been found to decrease levels of MDA and 8-hydroxy-2'-deoxyguanosine (8OH-dG) in the hippocampus and cortex, as well as reduce caspase-3 activity, inhibit microglial activation, and decrease infarct size in P7 Sprague-Dawley rat pups when evaluated 24 hours after HII [19]. However, this hyperacute effect of SFN should be further studied to elucidate whether the mechanism is Nrf2 dependent.

In conclusion, our findings show that SFN has a protective effect on the immature brain affected by hypoxic-ischemic insult. Pretreatment with SFN was able to improve impaired hippocampal glucose uptake resulting in neuroprotection of the ischemic hippocampus. SFN should be thus considered as a potent neuroprotective drug with the capability to interfere with pathophysiological processes triggered by perinatal hypoxic-ischemic insult. However, its potential use in clinical practice will require further studies especially targeted on the application scheme of Nrf2 activation.

Conflict of Interest

There is no conflict of interest.

Acknowledgments

The project was supported by Czech Science Foundation grants no. 18-07908S and 22-28265S. Additional support of the IPHYS μ CT/PET facility within the MEYS CR was by Large RI Project LM2018129 Czech-Biolmaging. Dr. Brnoliaková has been supported by grants VEGA 02/0104/21 and APVV - 18 – 0336. We would like to express our thanks to Eva Lažková, Karla Bohunová, and Roman Liška for their excellent technical assistance.

References

1. Allen KA, Brandon DH. Hypoxic Ischemic Encephalopathy: Pathophysiology and Experimental Treatments. *Newborn and Infant Nursing Reviews*. 2011;11(3):125-133.
2. Bryce J, Boschi-Pinto C, Shibuya K, Black RE. WHO estimates the causes of death in children. *Lancet*. 2005;365(9465):1147-1152.
3. Edwards AB, Anderton RS, Knuckey NW, Meloni BP. Perinatal hypoxic-ischemic encephalopathy and neuroprotective peptide therapies: A case for cationic arginine-rich peptides (CARPs). *Brain Sciences*. 2018;8(8):15-20.
4. Glass HC, Shellhaas RA. Acute Symptomatic Seizures in Neonates. *Seminars in Pediatric Neurology*. 2019;32(3):183-190.
5. Varghese B, Xavier R, Manoj VC, et al. Magnetic resonance imaging spectrum of perinatal hypoxic-ischemic brain injury. *Indian Journal of Radiology and Imaging*. 2016;26(3):316-327.
6. Rocha-Ferreira E, Hristova M. Plasticity in the neonatal brain following hypoxic-ischaemic injury. *Neural Plasticity*. 2016; 2016: 4901014
7. Aslam HM Muhammad, Saleem S, Afzal R, et al. "Risk factors of birth asphyxia." *Italian journal of pediatrics*. 2014;40:94.
8. Perlman JM. Pathogenesis of hypoxic-ischemic brain injury. *Journal of Perinatology*. 2007;27:S39-S46.
9. Graham EM, Burd I, Everett AD, Northington FJ. Blood biomarkers for evaluation of perinatal encephalopathy. *Frontiers in Pharmacology*. 2016;7(JUL):1-12.
10. Yang SN, Lai MC. Perinatal hypoxic-ischemic encephalopathy. *Journal of Biomedicine and Biotechnology*. 2011; 2011: 609813
11. Patel M. Mitochondrial dysfunction and oxidative stress: Cause and consequence of epileptic seizures. *Free Radical Biology and Medicine*. 2004;37(12):1951-1962.
12. Lin MT, Beal MF. Mitochondrial dysfunction and oxidative stress in neurodegenerative diseases. *Nature*. 2006;443(7113):787-795.
13. Rowley S, Patel M. Mitochondrial involvement and oxidative stress in temporal lobe epilepsy. *Free Radical Biology and Medicine*. 2013;62:121-131.
14. Folbergrová J, Ješina P, Kubová N, Druga R, Otáhal J. Status epilepticus in immature rats is associated with oxidative stress and mitochondrial dysfunction. *Frontiers in Cellular Neuroscience*. 2016;10(MAY):136.
15. Bhat AH, Dar KB, Anees S, et al. Oxidative stress, mitochondrial dysfunction and neurodegenerative diseases; a mechanistic insight. *Biomedicine and Pharmacotherapy*. 2015;74:101-110.
16. Qin X, Cheng J, Zhong Y, et al. Mechanism and treatment related to oxidative stress in neonatal hypoxic-ischemic encephalopathy. *Frontiers in Molecular Neuroscience*. 2019;12(April):1-10.

17. Bouayed J, Bohn T. Exogenous antioxidants - Double-edged swords in cellular redox state: Health beneficial effects at physiologic doses versus deleterious effects at high doses. *Oxidative Medicine and Cellular Longevity*. 2010;3(4):228-237.
18. Mattson MP, Gleichmann M, Cheng A. Mitochondria in Neuroplasticity and Neurological Disorders. *Neuron*. 2008;60(5):748-766.
19. Ping Z, Liu W, Kang Z, et al. Sulforaphane protects brains against hypoxic-ischemic injury through induction of Nrf2-dependent phase 2 enzyme. *Brain Research*. 2010;1343:178-185.
20. Tarozzi A, Angeloni C, Malaguti M, Morroni F, Hrelia S, Hrelia P. Sulforaphane as a Potential protective phytochemical against neurodegenerative diseases. *Oxid Med Cell Longev*. 2013; 2013: 415078.
21. O'Mealey GB, Berry WL, Plafker SM. Sulforaphane is a Nrf2-independent inhibitor of mitochondrial fission. *Redox Biology*. 2017;11(November 2016):103-110.
22. Kubo E, Chhunchha B, Singh P, Sasaki H, Singh DP. Sulforaphane reactivates cellular antioxidant defense by inducing Nrf2/ARE/Prdx6 activity during aging and oxidative stress. *Scientific Reports*. 2017;7(1):1-17.
23. Heiss EH, Schachner D, Zimmermann K, Dirsch VM. Glucose availability is a decisive factor for Nrf2-mediated gene expression. *Redox Biology*. 2013;1(1):359-365.
24. Ma Q. Role of Nrf2 in oxidative stress and toxicity. *Annual Review of Pharmacology and Toxicology*. 2013;53:401-426.
25. Tonelli C, Chio IIC, Tuveson DA. Transcriptional Regulation by Nrf2. *Antioxidants and Redox Signaling*. 2018;29(17):1727-1745.
26. Zhang Y, Gilmour A, Ahn Y hoon, De L. Phytomedicine The isothiocyanate sulforaphane inhibits mTOR in an NRF2-independent manner. 2021;86(May 2019):2-7.
27. Alfieri A, Srivastava S, Siow RCM, Modo M, Fraser PA, Giovanni E. Targeting the Nrf2 – Keap1 antioxidant defence pathway for neurovascular protection in stroke. 2011;17(April):4125-4136.
28. Pfister RH, Soll RF. Hypothermia for the treatment of infants with hypoxic-ischemic encephalopathy. *Journal of Perinatology*. 2010;30(SUPPL. 1):82-87.
29. Shah PS, Ohlsson A, Perlman M. Hypothermia to treat neonatal hypoxic ischemic encephalopathy: Systematic review. *Obstetrical and Gynecological Survey*. 2008;63(2):85-86.
30. Frajewicki A, Laštůvka Z, Borbélyová V, et al. Perinatal hypoxic-ischemic damage: review of the current treatment possibilities. *Physiological research*. 2021;69:S379-S401.
31. Semple BD, Blomgren K, Gimlin K, Ferriero DM, Noble-Haeusslein LJ. Brain development in rodents and humans: Identifying benchmarks of maturation and vulnerability to injury across species. *Progress in Neurobiology*. 2013; 106-107: 1-16.
32. Vannucci RC, Vannucci SJ. Perinatal hypoxic-ischemic brain damage: Evolution of an animal model. *Developmental Neuroscience*. 2005;27:81–86
33. Ismet S. PET studies in epilepsy. *Am J Nucl Med Mol Imaging*. 2015;5(5):416-430.

34. Schiffer WK, Mirrione MM, Biegon A, Alexoff DL, Patel V, Dewey SL. Serial microPET measures of the metabolic reaction to a microdialysis probe implant. *Journal of Neuroscience Methods*. 2006;155(2):272-284.
35. Sánchez F, Orero A, Soriano A. ALBIRA : A small animal PET / SPECT / CT imaging system. 2013;40(5):1-11.
36. Metz GA, Whishaw IQ. The ladder rung walking task: A scoring system and its practical application. *Journal of Visualized Experiments*. 2009;(28):2-5.
37. Dinkova-Kostova AT, Kostov R V. Glucosinolates and isothiocyanates in health and disease. *Trends in Molecular Medicine*. 2012;18(6):337-347.
38. De Lange C, Malinen E, Qu H, et al. Dynamic FDG PET for assessing early effects of cerebral hypoxia and resuscitation in new-born pigs. *European Journal of Nuclear Medicine and Molecular Imaging*. 2012;39(5):792-799.
39. Gilland E, Bona E, Hagberg H. Temporal changes of regional glucose use, blood flow, and microtubule-associated protein 2 immunostaining after hypoxia-ischemia in the immature rat brain. *Journal of Cerebral Blood Flow and Metabolism*. 1998;18(2):222-228.
40. Vannucci RC, Yager JY, Vannucci SJ. Cerebral glucose and energy utilization during the evolution of hypoxic-ischemic brain damage in the immature rat. *Journal of Cerebral Blood Flow and Metabolism*. 1994;14(2):279-288.
41. Thorngren-Jerneck K, Ohlsson T, Sandell A, et al. Cerebral glucose metabolism measured by positron emission tomography in term newborn infants with hypoxic ischemic encephalopathy. *Pediatric Research*. 2001;49(4):495-501.
42. Svoboda J, Litvinec A, Kala D, et al. Strain differences in intraluminal thread model of middle cerebral artery occlusion in rats. *Physiological Research*. 2019;68(1):37-48.
43. Laštůvka Z, Borbélyová V, Janišová K, Otáhal J, Mysliveček J, Riljak V. Neonatal Hypoxic-Ischemic Brain Injury Leads to Sex-Specific Deficits in Rearing and Climbing in Adult Mice. *Physiological Research*. 2020;69:S499-S512.
44. Lubics A, Reglodi D, Tamás A, et al. Neurological reflexes and early motor behavior in rats subjected to neonatal hypoxic-ischemic injury. *Behavioural Brain Research*. 2005;157(1):157-165
45. Goodfellow MJ, Borcar A, Proctor JL, Greco T, Rosenthal RE, Fiskum G. Transcriptional activation of antioxidant gene expression by Nrf2 protects against mitochondrial dysfunction and neuronal death associated with acute and chronic neurodegeneration. *Experimental Neurology*. 2020;328:113247.
46. Guerrero-Beltrán CE, Calderón-Oliver M, Pedraza-Chaverri J, Chirino YI. Protective effect of sulforaphane against oxidative stress: Recent advances. *Experimental and Toxicologic Pathology*. 2012;64(5):503-508.
47. Ma LL, Xing GP, Yu Y, et al. Exerts neuroprotective effects via suppression of the inflammatory response in a rat model of focal cerebral ischemia. *International Journal of Clinical and Experimental Medicine*. 2015;8(10):17811-17817.

48. Zhao X, Sun G, Zhang J, et al. Transcription factor Nrf2 protects the brain from damage produced by intracerebral hemorrhage. *Stroke*. 2007;38(12):3280-3286.
49. Daněk J, Danačíková Š, Kala D, Svoboda J, Kapoor S, Kapoor S, Pošusta A, Folbergrová J, Tauchmannová K, Mráček T and Otáhal J. Sulforaphane Ameliorates Metabolic Changes Associated With Status Epilepticus in Immature Rats. *Front. Cell. Neurosci.* 2022; 16:855161. doi: 10.3389/fncel.2022.855161